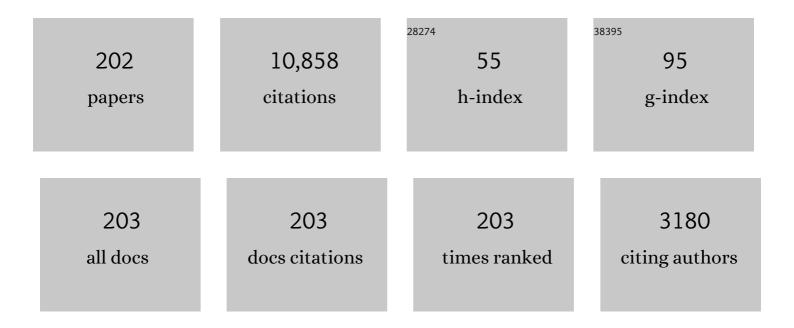
List of Publications by Year in descending order

Source: https://exaly.com/author-pdf/3201312/publications.pdf Version: 2024-02-01



XINI IN LI

#	Article	IF	CITATIONS
1	Science Goals and Overview of the Radiation Belt Storm Probes (RBSP) Energetic Particle, Composition, and Thermal Plasma (ECT) Suite on NASA's Van Allen Probes Mission. Space Science Reviews, 2013, 179, 311-336.	8.1	463
2	The Electric Field and Waves Instruments on the Radiation Belt Storm Probes Mission. Space Science Reviews, 2013, 179, 183-220.	8.1	421
3	Simulation of the prompt energization and transport of radiation belt particles during the March 24, 1991 SSC. Geophysical Research Letters, 1993, 20, 2423-2426.	4.0	393
4	The Relativistic Electron-Proton Telescope (REPT) Instrument on Board the Radiation Belt Storm Probes (RBSP) Spacecraft: Characterization of Earth's Radiation Belt High-Energy Particle Populations. Space Science Reviews, 2013, 179, 337-381.	8.1	334
5	An extreme distortion of the Van Allen belt arising from the â€~Hallowe'en' solar storm in 2003. Nature, 2004, 432, 878-881.	27.8	299
6	Multisatellite observations of the outer zone electron variation during the November 3–4, 1993, magnetic storm. Journal of Geophysical Research, 1997, 102, 14123-14140.	3.3	274
7	Energetic electron response to ULF waves induced by interplanetary shocks in the outer radiation belt. Journal of Geophysical Research, 2009, 114, .	3.3	266
8	Quantitative prediction of radiation belt electrons at geostationary orbit based on solar wind measurements. Geophysical Research Letters, 2001, 28, 1887-1890.	4.0	232
9	A Long-Lived Relativistic Electron Storage Ring Embedded in Earth's Outer Van Allen Belt. Science, 2013, 340, 186-190.	12.6	216
10	Source and seed populations for relativistic electrons: Their roles in radiation belt changes. Journal of Geophysical Research: Space Physics, 2015, 120, 7240-7254.	2.4	215
11	Simulation of dispersionless injections and drift echoes of energetic electrons associated with substorms. Geophysical Research Letters, 1998, 25, 3763-3766.	4.0	199
12	A major solar eruptive event in July 2012: Defining extreme space weather scenarios. Space Weather, 2013, 11, 585-591.	3.7	189
13	A new model for the prediction ofDston the basis of the solar wind. Journal of Geophysical Research, 2002, 107, SMP 31-1-SMP 31-8.	3.3	166
14	Ultralow frequency modulation of energetic particles in the dayside magnetosphere. Geophysical Research Letters, 2007, 34, .	4.0	163
15	An impenetrable barrier to ultrarelativistic electrons in the Van Allen radiation belts. Nature, 2014, 515, 531-534.	27.8	159
16	Long term measurements of radiation belts by SAMPEX and their variations. Geophysical Research Letters, 2001, 28, 3827-3830.	4.0	154
17	The Electron Radiation Belt. Space Science Reviews, 2001, 95, 569-580.	8.1	145
18	Coronal mass ejections, magnetic clouds, and relativistic magnetospheric electron events: ISTP. Journal of Geophysical Research, 1998, 103, 17279-17291.	3.3	144

#	Article	IF	CITATIONS
19	Simulation of energetic particle injections associated with a substorm on August 27, 2001. Geophysical Research Letters, 2003, 30, 4-1-4-4.	4.0	140
20	Recurrent geomagnetic storms and relativistic electron enhancements in the outer magnetosphere: ISTP coordinated measurements. Journal of Geophysical Research, 1997, 102, 14141-14148.	3.3	133
21	Gradual diffusion and punctuated phase space density enhancements of highly relativistic electrons: Van Allen Probes observations. Geophysical Research Letters, 2014, 41, 1351-1358.	4.0	127
22	Dstmodel for 1995–2002. Journal of Geophysical Research, 2006, 111, .	3.3	126
23	Correlation between the inner edge of outer radiation belt electrons and the innermost plasmapause location. Geophysical Research Letters, 2006, 33, .	4.0	119
24	A strong CME-related magnetic cloud interaction with the Earth's Magnetosphere: ISTP observations of rapid relativistic electron acceleration on May 15, 1997. Geophysical Research Letters, 1998, 25, 2975-2978.	4.0	118
25	Energetic electrons, 50 keV to 6 MeV, at geosynchronous orbit: Their responses to solar wind variations. Space Weather, 2005, 3, n/a-n/a.	3.7	112
26	Are energetic electrons in the solar wind the source of the outer radiation belt?. Geophysical Research Letters, 1997, 24, 923-926.	4.0	110
27	Observations of coincident EMIC wave activity and duskside energetic electron precipitation on 18–19 January 2013. Geophysical Research Letters, 2015, 42, 5727-5735.	4.0	102
28	Simulation of proton radiation belt formation during the March 24, 1991 SSC. Geophysical Research Letters, 1995, 22, 291-294.	4.0	98
29	Highly relativistic radiation belt electron acceleration, transport, and loss: Large solar storm events of March and June 2015. Journal of Geophysical Research: Space Physics, 2016, 121, 6647-6660.	2.4	93
30	Variations of 0.7-6.0 MeV electrons at geosynchronous orbit as a function of solar wind. Space Weather, 2004, 2, n/a-n/a.	3.7	92
31	On the calculation of electric diffusion coefficient of radiation belt electrons with in situ electric field measurements by THEMIS. Geophysical Research Letters, 2016, 43, 1023-1030.	4.0	90
32	Simulation of the 23 July 2012 extreme space weather event: What if this extremely rare CME was Earth directed?. Space Weather, 2013, 11, 671-679.	3.7	87
33	Pitch angle distribution analysis of radiation belt electrons based on Combined Release and Radiation Effects Satellite Medium Electrons A data. Journal of Geophysical Research, 2007, 112, n/a-n/a.	3.3	86
34	Modeling energetic particle injections in dynamic pulse fields with varying propagation speeds. Journal of Geophysical Research, 2002, 107, SMP 1-1.	3.3	85
35	Strong electron acceleration in the Earth's magnetosphere. Advances in Space Research, 1998, 21, 609-613.	2.6	83
36	Understanding the Mechanisms of Radiation Belt Dropouts Observed by Van Allen Probes. Journal of Geophysical Research: Space Physics, 2017, 122, 9858-9879.	2.4	83

#	Article	IF	CITATIONS
37	Particle Dynamics in the Earth's Radiation Belts: Review of Current Research and Open Questions. Journal of Geophysical Research: Space Physics, 2020, 125, e2019JA026735.	2.4	81
38	Electric and magnetic field observations of Pc4 and Pc5 pulsations in the inner magnetosphere: A statistical study. Journal of Geophysical Research, 2009, 114, .	3.3	79
39	Stormâ€dependent radiation belt electron dynamics. Journal of Geophysical Research, 2009, 114, .	3.3	78
40	Upper limit on the inner radiation belt MeV electron intensity. Journal of Geophysical Research: Space Physics, 2015, 120, 1215-1228.	2.4	77
41	Poloidal ULF wave observed in the plasmasphere boundary layer. Journal of Geophysical Research: Space Physics, 2013, 118, 4298-4307.	2.4	74
42	The evolution of ring current ion energy density and energy content during geomagnetic storms based on Van Allen Probes measurements. Journal of Geophysical Research: Space Physics, 2015, 120, 7493-7511.	2.4	70
43	Rapid MeV electron precipitation as observed by SAMPEX/HILT during highâ€speed streamâ€driven storms. Journal of Geophysical Research: Space Physics, 2015, 120, 3783-3794.	2.4	70
44	Prompt acceleration of magnetospheric electrons to ultrarelativistic energies by the 17 March 2015 interplanetary shock. Journal of Geophysical Research: Space Physics, 2016, 121, 7622-7635.	2.4	68
45	Behavior of MeV electrons at geosynchronous orbit during last two solar cycles. Journal of Geophysical Research, 2011, 116, n/a-n/a.	3.3	66
46	Plasmaspheric hiss waves generate a reversed energy spectrum of radiation belt electrons. Nature Physics, 2019, 15, 367-372.	16.7	66
47	Ponderomotive effects on ion acceleration in the auroral zone. Geophysical Research Letters, 1993, 20, 13-16.	4.0	65
48	First results from CSSWE CubeSat: Characteristics of relativistic electrons in the nearâ€Earth environment during the October 2012 magnetic storms. Journal of Geophysical Research: Space Physics, 2013, 118, 6489-6499.	2.4	65
49	Quantifying radial diffusion coefficients of radiation belt electrons based on global MHD simulation and spacecraft measurements. Journal of Geophysical Research, 2012, 117, .	3.3	62
50	Nearâ€Earth injection of MeV electrons associated with intense dipolarization electric fields: Van Allen Probes observations. Geophysical Research Letters, 2015, 42, 6170-6179.	4.0	62
51	Quantification of the precipitation loss of radiation belt electrons observed by SAMPEX. Journal of Geophysical Research, 2010, 115, .	3.3	61
52	Energetic particle injections in the inner magnetosphere as a response to an interplanetary shock. Journal of Atmospheric and Solar-Terrestrial Physics, 2003, 65, 233-244.	1.6	60
53	Observations of the impenetrable barrier, the plasmapause, and the VLF bubble during the 17 March 2015 storm. Journal of Geophysical Research: Space Physics, 2016, 121, 5537-5548.	2.4	59
54	Modeling the radiation belt electrons with radial diffusion driven by the solar wind. Space Weather, 2005, 3, n/a-n/a.	3.7	58

#	Article	IF	CITATIONS
55	Characteristics of middle―to lowâ€latitude Pi2 excited by bursty bulk flows. Journal of Geophysical Research, 2008, 113, .	3.3	58
56	Formation of intense nose structures. Geophysical Research Letters, 2001, 28, 491-494.	4.0	55
57	Energetic electron injections into the inner magnetosphere during the Jan. 10-11, 1997 magnetic storm. Geophysical Research Letters, 1998, 25, 2561-2564.	4.0	53
58	Peculiar pitch angle distribution of relativistic electrons in the inner radiation belt and slot region. Geophysical Research Letters, 2014, 41, 2250-2257.	4.0	53
59	Quantitative forecast of relativistic electron flux at geosynchronous orbit based on lowâ€energy electron flux. Space Weather, 2008, 6, .	3.7	52
60	Statistical roles of storms and substorms in changing the entire outer zone relativistic electron population. Journal of Geophysical Research, 2009, 114, .	3.3	52
61	Modeling energetic electron penetration into the slot region and inner radiation belt. Journal of Geophysical Research: Space Physics, 2013, 118, 6936-6945.	2.4	52
62	Ring current electron dynamics during geomagnetic storms based on the Van Allen Probes measurements. Journal of Geophysical Research: Space Physics, 2016, 121, 3333-3346.	2.4	52
63	Modeling of 1–2 September 1859 super magnetic storm. Advances in Space Research, 2006, 38, 273-279.	2.6	50
64	Inward shift of outer radiation belt electrons as a function of <i>Dst</i> index and the influence of the solar wind on electron injections into the slot region. Journal of Geophysical Research: Space Physics, 2013, 118, 756-764.	2.4	50
65	Observations of the inner radiation belt: CRAND and trapped solar protons. Journal of Geophysical Research: Space Physics, 2014, 119, 6541-6552.	2.4	50
66	Dynamic plasmapause model based on THEMIS measurements. Journal of Geophysical Research: Space Physics, 2015, 120, 10,543.	2.4	50
67	Measurement of electrons from albedo neutron decay and neutron density in near-Earth space. Nature, 2017, 552, 382-385.	27.8	50
68	Fast Diffusion of Ultrarelativistic Electrons in the Outer Radiation Belt: 17 March 2015 Storm Event. Geophysical Research Letters, 2018, 45, 10874-10882.	4.0	49
69	Multiyear Measurements of Radiation Belt Electrons: Acceleration, Transport, and Loss. Journal of Geophysical Research: Space Physics, 2019, 124, 2588-2602.	2.4	48
70	Rapid enchancements of relativistic electrons deep in the magnetosphere during the May 15, 1997, magnetic storm. Journal of Geophysical Research, 1999, 104, 4467-4476.	3.3	47
71	A nonstorm time enhancement of relativistic electrons in the outer radiation belt. Geophysical Research Letters, 2014, 41, 7-12.	4.0	47
72	Roles of whistler mode waves and magnetosonic waves in changing the outer radiation belt and the slot region. Journal of Geophysical Research: Space Physics, 2017, 122, 5431-5448.	2.4	47

#	Article	IF	CITATIONS
73	Solar wind influence on Pc4 and Pc5 ULF wave activity in the inner magnetosphere. Journal of Geophysical Research, 2010, 115, .	3.3	46
74	Miniature X-Ray Solar Spectrometer: A Science-Oriented, University 3U CubeSat. Journal of Spacecraft and Rockets, 2016, 53, 328-339.	1.9	46
75	New conjunctive CubeSat and balloon measurements to quantify rapid energetic electron precipitation. Geophysical Research Letters, 2013, 40, 5833-5837.	4.0	43
76	Variability of the pitch angle distribution of radiation belt ultrarelativistic electrons during and following intense geomagnetic storms: Van Allen Probes observations. Journal of Geophysical Research: Space Physics, 2015, 120, 4863-4876.	2.4	43
77	Propagation characteristics of plasmaspheric hiss: Van Allen Probe observations and global empirical models. Journal of Geophysical Research: Space Physics, 2017, 122, 4156-4167.	2.4	43
78	Characteristics of pitch angle distributions of hundreds of keV electrons in the slot region and inner radiation belt. Journal of Geophysical Research: Space Physics, 2014, 119, 9543-9557.	2.4	41
79	An Empirical Model of Radiation Belt Electron Pitch Angle Distributions Based On Van Allen Probes Measurements. Journal of Geophysical Research: Space Physics, 2018, 123, 3493-3511.	2.4	41
80	Parametric Sensitivity of the Formation of Reversed Electron Energy Spectrum Caused by Plasmaspheric Hiss. Geophysical Research Letters, 2019, 46, 4134-4143.	4.0	41
81	Simulating radial diffusion of energetic (MeV) electrons through a model of fluctuating electric and magnetic fields. Annales Geophysicae, 2006, 24, 2583-2598.	1.6	39
82	Modeling the deep penetration of outer belt electrons during the "Halloween―magnetic storm in 2003. Space Weather, 2009, 7, .	3.7	39
83	On phase space density radial gradients of Earth's outerâ€belt electrons prior to sudden solar wind pressure enhancements: Results from distinctive events and a superposed epoch analysis. Journal of Geophysical Research, 2010, 115, .	3.3	38
84	On the relation between radiation belt electrons and solar wind parameters/geomagnetic indices: Dependence on the first adiabatic invariant and <i>L</i> [*] . Journal of Geophysical Research: Space Physics, 2017, 122, 1624-1642.	2.4	38
85	High resolution patterning of Ag nanowire flexible transparent electrode via electrohydrodynamic jet printing of acrylic polymer-silicate nanoparticle composite overcoating layer. Organic Electronics, 2018, 62, 400-406.	2.6	37
86	THEMIS observations of the spatial extent and pressureâ€pulse excitation of field line resonances. Geophysical Research Letters, 2010, 37, .	4.0	36
87	Prediction of the <i>AU</i> , <i>AL</i> , and <i>AE</i> indices using solar wind parameters. Journal of Geophysical Research: Space Physics, 2013, 118, 7683-7694.	2.4	36
88	Prediction of theALindex using solar wind parameters. Journal of Geophysical Research, 2007, 112, n/a.	3.3	35
89	Radiation belt electron dynamics at low <i>L</i> (<4): Van Allen Probes era versus previous two solar cycles. Journal of Geophysical Research: Space Physics, 2017, 122, 5224-5234.	2.4	33
90	Direct writing of silver nanowire electrodes via dragging mode electrohydrodynamic jet printing for organic thin film transistors. Organic Electronics, 2018, 62, 357-365.	2.6	33

#	Article	IF	CITATIONS
91	Occurrence characteristics of outer zone relativistic electron butterfly distribution: A survey of Van Allen Probes REPT measurements. Geophysical Research Letters, 2016, 43, 5644-5652.	4.0	32
92	Large-amplitude electric fields in the inner magnetosphere: Van Allen Probes observations of subauroral polarization streams. Journal of Geophysical Research: Space Physics, 2016, 121, 5294-5306.	2.4	32
93	Prompt injections of highly relativistic electrons induced by interplanetary shocks: A statistical study of Van Allen Probes observations. Geophysical Research Letters, 2016, 43, 12,317.	4.0	32
94	Cone-jet printing of aligned silver nanowire/poly(ethylene oxide) composite electrodes for organic thin-film transistors. Organic Electronics, 2019, 69, 190-199.	2.6	32
95	Characteristics of 2–6 MeV electrons in the slot region and inner radiation belt. Journal of Geophysical Research, 2006, 111, .	3.3	31
96	Radial gradients of phase space density of the outer radiation belt electrons prior to sudden solar wind pressure enhancements. Geophysical Research Letters, 2008, 35, .	4.0	31
97	The Relativistic Electron-Proton Telescope (REPT) Instrument on Board the Radiation Belt Storm Probes (RBSP) Spacecraft: Characterization of Earth's Radiation Belt High-Energy Particle Populations. , 2012, , 337-381.		31
98	Multiple discrete-energy ion features in the inner magnetosphere: Observations and simulations. Geophysical Research Letters, 2000, 27, 1447-1450.	4.0	29
99	Parametric study of shock-induced transport and energization of relativistic electrons in the magnetosphere. Journal of Geophysical Research, 2005, 110, .	3.3	29
100	Joint responses of geosynchronous magnetic field and relativistic electrons to external changes in solar wind dynamic pressure and interplanetary magnetic field. Journal of Geophysical Research: Space Physics, 2013, 118, 1472-1482.	2.4	29
101	THEMIS measurements of quasiâ€static electric fields in the inner magnetosphere. Journal of Geophysical Research: Space Physics, 2014, 119, 9939-9951.	2.4	29
102	Evolution of relativistic outer belt electrons during an extended quiescent period. Journal of Geophysical Research: Space Physics, 2014, 119, 9558-9566.	2.4	28
103	Characteristics of the ion pressure tensor in the Earth's magnetosheath. Geophysical Research Letters, 1995, 22, 667-670.	4.0	27
104	The effect of surfactants on electrohydrodynamic jet printing and the performance of organic field-effect transistors. Physical Chemistry Chemical Physics, 2018, 20, 1210-1220.	2.8	27
105	On the Acceleration Mechanism of Ultrarelativistic Electrons in the Center of the Outer Radiation Belt: A Statistical Study. Journal of Geophysical Research: Space Physics, 2019, 124, 8590-8599.	2.4	27
106	Relativistic Electron Model in the Outer Radiation Belt Using a Neural Network Approach. Space Weather, 2021, 19, e2021SW002808.	3.7	27
107	Multi-satellite simultaneous observations of magnetopause and atmospheric losses of radiation belt electrons during an intense solar wind dynamic pressure pulse. Annales Geophysicae, 2016, 34, 493-509.	1.6	26
108	Inward diffusion and loss of radiation belt protons. Journal of Geophysical Research: Space Physics, 2016, 121, 1969-1978.	2.4	26

#	Article	IF	CITATIONS
109	Modeling the Quasiâ€Trapped Electron Fluxes From Cosmic Ray Albedo Neutron Decay (CRAND). Geophysical Research Letters, 2019, 46, 1919-1928.	4.0	26
110	Multiple responses of magnetotail to the enhancement and fluctuation of solar wind dynamic pressure and the southward turning of interplanetary magnetic field. Journal of Geophysical Research, 2011, 116, n/a-n/a.	3.3	25
111	The role of the convection electric field in filling the slot region between the inner and outer radiation belts. Journal of Geophysical Research: Space Physics, 2017, 122, 2051-2068.	2.4	25
112	The Acceleration of Ultrarelativistic Electrons During a Small to Moderate Storm of 21 April 2017. Geophysical Research Letters, 2018, 45, 5818-5825.	4.0	25
113	Characterization and Evolution of Radiation Belt Electron Energy Spectra Based on the Van Allen Probes Measurements. Journal of Geophysical Research: Space Physics, 2019, 124, 4217-4232.	2.4	25
114	The Effects of Geomagnetic Storms and Solar Wind Conditions on the Ultrarelativistic Electron Flux Enhancements. Journal of Geophysical Research: Space Physics, 2019, 124, 1948-1965.	2.4	25
115	Cosmic Ray Albedo Neutron Decay (CRAND) as a Source of Inner Belt Electrons: Energy Spectrum Study. Geophysical Research Letters, 2019, 46, 544-552.	4.0	25
116	Evolution of the dispersionless injection boundary associated with substorms. Annales Geophysicae, 2005, 23, 877-884.	1.6	24
117	Mode number calculations of ULF fieldâ€line resonances using ground magnetometers and THEMIS measurements. Journal of Geophysical Research: Space Physics, 2013, 118, 6986-6997.	2.4	24
118	Compression-amplified EMIC waves and their effects on relativistic electrons. Physics of Plasmas, 2016, 23, .	1.9	24
119	Electrohydrodynamic (EHD) jet printing of carbon-black composites for solution-processed organic field-effect transistors. Organic Electronics, 2019, 73, 279-285.	2.6	24
120	Non-lithographic direct patterning of carbon nanomaterial electrodes via electrohydrodynamic-printed wettability patterns by polymer brush for fabrication of organic field-effect transistor. Applied Surface Science, 2020, 515, 145989.	6.1	24
121	On the relationship between electron flux oscillations and ULF waveâ€driven radial transport. Journal of Geophysical Research: Space Physics, 2017, 122, 9306-9319.	2.4	23
122	Effect of Lowâ€Harmonic Magnetosonic Waves on the Radiation Belt Electrons Inside the Plasmasphere. Journal of Geophysical Research: Space Physics, 2019, 124, 3390-3401.	2.4	23
123	The Relativistic Electron-Proton Telescope (REPT) Investigation: Design, Operational Properties, and Science Highlights. Space Science Reviews, 2021, 217, 1.	8.1	23
124	Rapid loss of the plasma sheet energetic electrons associated with the growth of whistler mode waves inside the bursty bulk flows. Journal of Geophysical Research: Space Physics, 2013, 118, 7200-7210.	2.4	22
125	Van Allen Probes Measurements of Energetic Particle Deep Penetration Into the Low L Region (<i>L</i> Â<Â4) During the Storm on 8 April 2016. Journal of Geophysical Research: Space Physics, 2017, 122, 12,140.	2.4	22
126	Modeling the Proton Radiation Belt With Van Allen Probes Relativistic Electronâ€Proton Telescope Data. Journal of Geophysical Research: Space Physics, 2018, 123, 685-697.	2.4	22

#	Article	IF	CITATIONS
127	The <i>Dst</i> index underestimates the solar cycle variation of geomagnetic activity. Journal of Geophysical Research: Space Physics, 2015, 120, 5603-5607.	2.4	21
128	Observations at geosynchronous orbit of a persistent Pc5 geomagnetic pulsation and energetic electron flux modulations. Annales Geophysicae, 2007, 25, 1653-1667.	1.6	20
129	Observations and analysis of Alfvén wave phase mixing in the Earth's magnetosphere. Journal of Geophysical Research, 2009, 114, .	3.3	20
130	On the Initial Enhancement of Energetic Electrons and the Innermost Plasmapause Locations: Coronal Mass Ejectionâ€Ðriven Storm Periods. Journal of Geophysical Research: Space Physics, 2018, 123, 9252-9264.	2.4	20
131	Colorado Student Space Weather Experiment: Differential Flux Measurements of Energetic Particles in a Highly Inclined Low Earth Orbit. Geophysical Monograph Series, 0, , 385-404.	0.1	19
132	Small Mission Accomplished by Students—Big Impact on Space Weather Research. Space Weather, 2013, 11, 55-56.	3.7	19
133	On Energetic Electron Dynamics During Geomagnetic Quiet Times in Earth's Inner Radiation Belt due to Atmospheric Collisional Loss and CRAND as a Source. Journal of Geophysical Research: Space Physics, 2020, 125, e2019JA027678.	2.4	19
134	Direct-patterned copper/poly(ethylene oxide) composite electrodes for organic thin-film transistors through cone-jet mode by electrohydrodynamic jet printing. Journal of Industrial and Engineering Chemistry, 2020, 85, 269-275.	5.8	19
135	Energetic plasma sheet electrons and their relationship with the solar wind: A Cluster and Geotail study. Journal of Geophysical Research, 2009, 114, .	3.3	18
136	Simultaneous eventâ€specific estimates of transport, loss, and source rates for relativistic outer radiation belt electrons. Journal of Geophysical Research: Space Physics, 2017, 122, 3354-3373.	2.4	18
137	The Rapid Responses of Magnetosonic Waves to the Compression and Expansion of Earth's Magnetosphere. Geophysical Research Letters, 2017, 44, 11,239.	4.0	18
138	Spatial structure and temporal evolution of a dayside poloidal ULF wave event. Geophysical Research Letters, 2011, 38, n/a-n/a.	4.0	17
139	Relativistic electron response to the combined magnetospheric impact of a coronal mass ejection overlapping with a highâ€speed stream: Van Allen Probes observations. Journal of Geophysical Research: Space Physics, 2015, 120, 7629-7641.	2.4	17
140	Detailed characteristics of radiation belt electrons revealed by CSSWE/REPTile measurements: Geomagnetic activity response and precipitation observation. Journal of Geophysical Research: Space Physics, 2017, 122, 8434-8445.	2.4	16
141	Observations of Impulsive Electric Fields Induced by Interplanetary Shock. Geophysical Research Letters, 2018, 45, 7287-7296.	4.0	16
142	Comparison of Van Allen Probes Energetic Electron Data With Corresponding GOESâ€15 Measurements: 2012–2018. Journal of Geophysical Research: Space Physics, 2019, 124, 9924-9942.	2.4	16
143	Bounded anisotropy fluid model for ion temperature evolution applied to AMPTE/IRM magnetosheath data. Journal of Geophysical Research, 1995, 100, 14925.	3.3	15
144	Great geomagnetic storm of 9 November 1991: Association with a disappearing solar filament. Journal of Geophysical Research, 2009, 114, .	3.3	15

#	Article	IF	CITATIONS
145	Electron Diffusion by Coexisting Plasmaspheric Hiss and Chorus Waves: Multisatellite Observations and Simulations. Geophysical Research Letters, 2020, 47, e2020GL088753.	4.0	15
146	A parametric study of the source rate for outer radiation belt electrons using a Kalman filter. Journal of Geophysical Research, 2012, 117, .	3.3	14
147	Specification of >2 MeV geosynchronous electrons based on solar wind measurements. Space Weather, 2006, 4, n/a-n/a.	3.7	13
148	Statistical Relationship Between Exohiss Waves and Plasmaspheric Hiss. Geophysical Research Letters, 2020, 47, e2020GL087023.	4.0	13
149	Scalable fabrication of carbon materials based silicon rubber for highly stretchable e-textile sensor. Nanotechnology Reviews, 2020, 9, 1183-1191.	5.8	13
150	Using spacecraft measurements ahead of Earth in the Parker spiral to improve terrestrial space weather forecasts. Space Weather, 2011, 9, .	3.7	12
151	On energetic electrons (>38 keV) in the central plasma sheet: Data analysis and modeling. Journal of Geophysical Research, 2011, 116, n/a-n/a.	3.3	12
152	New technique to calculate electron Alfvén layer and its application in interpreting geosynchronous access of PS energetic electrons. Journal of Geophysical Research: Space Physics, 2015, 120, 1675-1683.	2.4	12
153	Relation Between Shockâ€Related Impulse and Subsequent ULF Wave in the Earth's Magnetosphere. Geophysical Research Letters, 2020, 47, e2020GL090027.	4.0	12
154	Effects of ULF waves on local and global energetic particles: Particle energy and species dependences. Journal of Geophysical Research: Space Physics, 2016, 121, 11,007.	2.4	11
155	Geomagnetic activity and local time dependence of the distribution of ultra low-frequency wave power in azimuthal wavenumbers, <i>m</i> . Annales Geophysicae, 2017, 35, 629-638.	1.6	11
156	The Effects of Solar Wind Dynamic Pressure Changes on the Substorm Auroras and Energetic Electron Injections on 24 August 2005. Journal of Geophysical Research: Space Physics, 2018, 123, 385-399.	2.4	11
157	Ultrawideband Rising‶one Chorus Waves Observed Inside the Oscillating Plasmapause. Journal of Geophysical Research: Space Physics, 2018, 123, 6670-6678.	2.4	11
158	Simulations of Electron Flux Oscillations as Observed by MagEIS in Response to Broadband ULF Waves. Journal of Geophysical Research: Space Physics, 2020, 125, e2020JA027798.	2.4	11
159	The predictability of the magnetosphere and space weather. Eos, 2003, 84, 361.	0.1	10
160	Adiabatic effects on radiation belt electrons at low altitude. Journal of Geophysical Research, 2011, 116, n/a-n/a.	3.3	10
161	Effect of carbon nanotube addition on mechanical reliability of Ag nanowire network. Materials Letters, 2017, 198, 202-205.	2.6	10
162	An improved forecast system for relativistic electrons at geosynchronous orbit. Space Weather, 2011, 9, .	3.7	9

#	Article	IF	CITATIONS
163	Facile method for enhancing conductivity of printed carbon nanotubes electrode via simple rinsing process. Organic Electronics, 2017, 47, 174-180.	2.6	9
164	Dynamics of Energetic Electrons in the Slot Region During Geomagnetically Quiet Times: Losses Due to Waveâ€Particle Interactions Versus a Source From Cosmic Ray Albedo Neutron Decay (CRAND). Journal of Geophysical Research: Space Physics, 2020, 125, e2020JA028042.	2.4	9
165	Modeling the Dynamics of Radiation Belt Electrons With Source and Loss Driven by the Solar Wind. Journal of Geophysical Research: Space Physics, 2021, 126, e2020JA028988.	2.4	9
166	Observation and simulation of the rapid formation of a new electron radiation belt during March 24, 1991 SSC. AIP Conference Proceedings, 1996, , .	0.4	8
167	Tailward leap of multiple expansions of the plasma sheet during a moderately intense substorm: THEMIS observations. Journal of Geophysical Research, 2012, 117, .	3.3	8
168	Sol–Gel-Processed Organic–Inorganic Hybrid for Flexible Conductive Substrates Based on Gravure-Printed Silver Nanowires and Graphene. Polymers, 2019, 11, 158.	4.5	8
169	How Sudden, Intense Energetic Electron Enhancements Correlate With the Innermost Plasmapause Locations Under Various Solar Wind Drivers and Geomagnetic Conditions. Journal of Geophysical Research: Space Physics, 2019, 124, 8992-9002.	2.4	8
170	On the Association Between Electron Flux Oscillations and Local Phase Space Density Gradients. Journal of Geophysical Research: Space Physics, 2021, 126, e2020JA028891.	2.4	8
171	Science Goals and Overview of the Radiation Belt Storm Probes (RBSP) Energetic Particle, Composition, and Thermal Plasma (ECT) Suite on NASA's Van Allen Probes Mission. , 2013, , 311-336.		8
172	Quasiâ€Trapped Electron Fluxes Induced by NWC Transmitter and CRAND: Observations and Simulations. Geophysical Research Letters, 2022, 49, .	4.0	8
173	The role of radial transport in accelerating radiation belt electrons. Geophysical Monograph Series, 2006, , 139-149.	0.1	7
174	Calculating ultra-low-frequency wave power of the compressional magnetic field vs. <i>L</i> and time: multi-spacecraft analysis using the Van Allen probes, THEMIS and GOES. Annales Geophysicae, 2016, 34, 565-571.	1.6	7
175	New Insights From Longâ€Term Measurements of Inner Belt Protons (10s of MeV) by SAMPEX, POES, Van Allen Probes, and Simulation Results. Journal of Geophysical Research: Space Physics, 2020, 125, e2020JA028198.	2.4	7
176	Equatorial Pitch Angle Distributions of 1–50ÂkeV Electrons in Earth's Inner Magnetosphere: An Empirical Model Based on the Van Allen Probes Observations. Journal of Geophysical Research: Space Physics, 2021, 126, .	2.4	7
177	Upper Limit of Electron Fluxes Observed in the Radiation Belts. Journal of Geophysical Research: Space Physics, 2021, 126, .	2.4	7
178	Van Allen Probes Observations of Multiâ€MeV Electron Driftâ€Periodic Flux Oscillations in Earth's Outer Radiation Belt During the March 2017 Event. Journal of Geophysical Research: Space Physics, 2021, 126, e2021JA029284.	2.4	7
179	Cluster observations of energetic electron flux variations within the plasma sheet. Journal of Geophysical Research, 2009, 114, .	3.3	6
180	Design and scientific return of a miniaturized particle telescope onboard the Colorado Student Space		6

Weather Experiment (CSSWE) CubeSat. , 2014, , .

#	Article	IF	CITATIONS
181	Evolution of the storm magnetic field disturbance around Earth's surface and the associated ring current as deduced from multiple ground observatories. Journal of Geophysical Research: Space Physics, 2015, 120, 564-580.	2.4	6
182	Competitive Influences of Different Plasma Waves on the Pitch Angle Distribution of Energetic Electrons Inside and Outside Plasmasphere. Geophysical Research Letters, 2022, 49, .	4.0	6
183	On the Challenges of Measuring Energetic Particles in the Inner Belt: A Geant4 Simulation of an Energetic Particle Detector Instrument, REPTileâ€2. Journal of Geophysical Research: Space Physics, 2022, 127, .	2.4	6
184	Dispersionless injection simulations explore auroral substorm origins. Eos, 1999, 80, 405.	0.1	5
185	Small Space Weather Research Mission Designed Fully by Students. Space Weather, 2011, 9, n/a-n/a.	3.7	5
186	The Dayâ€Night Difference and Geomagnetic Activity Variation of Energetic Electron Fluxes in Region of South Atlantic Anomaly. Space Weather, 2020, 18, e2020SW002479.	3.7	5
187	Complementary and Catalytic Roles of Manâ€Made VLF Waves and Natural Plasma Waves in the Loss of Radiation Belt Electrons. Journal of Geophysical Research: Space Physics, 2021, 126, e2020JA028879.	2.4	5
188	James Van Allen and His Namesake <scp>NASA</scp> Mission. Eos, 2013, 94, 469-470.	0.1	4
189	Longâ€Term Variations of Quasiâ€Trapped and Trapped Electrons in the Inner Radiation Belt Observed by DEMETER and SAMPEX. Journal of Geophysical Research: Space Physics, 2020, 125, e2020JA028086.	2.4	4
190	Achievements and Lessons Learned From Successful Small Satellite Missions for Space Weatherâ€Oriented Research. Space Weather, 2022, 20, .	3.7	4
191	Comparison of energetic electron flux and phase space density in the magnetosheath and in the magnetosphere. Journal of Geophysical Research, 2012, 117, .	3.3	3
192	Multiâ€Event Studies of Sudden Energetic Electron Enhancements in the Inner Magnetosphere and Its Association With Plasmapause Positions. Journal of Geophysical Research: Space Physics, 2021, 126, e2021JA029769.	2.4	3
193	Multiâ€MeV Electron Dynamics Near the Inner Edge of the Outer Radiation Belt. Geophysical Research Letters, 2021, 48, .	4.0	3
194	Ring Current Ion Interaction with Micropulsations. Geophysical Monograph Series, 0, , 469-476.	0.1	2
195	Statistics of Multiâ€MeV Electron Driftâ€Periodic Flux Oscillations Using Van Allen Probes Observations. Geophysical Research Letters, 2022, 49, .	4.0	2
196	Energy-dependent Boundaries of Earth's Radiation Belt Electron Slot Region. Astrophysical Journal, 2021, 922, 246.	4.5	2
197	Electron Phasespace Density Analysis Based on Test-Particle Simulations of Magnetospheric Compression Events. Geophysical Monograph Series, 2013, , 205-214.	0.1	1
198	One year of on-orbit performance of the Colorado Student Space Weather Experiment (CSSWE). , 2014, , \cdot		1

#	Article	IF	CITATIONS
199	Monitoring the global evolution of the storm ring current and storm indices from confined ground geomagnetic observatories. Journal of Atmospheric and Solar-Terrestrial Physics, 2019, 191, 105049.	1.6	1
200	Van Allen Belt Punctures and Their Correlation With Solar Wind, Geomagnetic Activity, and ULF Waves. Journal of Geophysical Research: Space Physics, 2021, 126, .	2.4	1
201	Determining the Location of the Dispersionless Injection Boundary During Substorms. AIP Conference Proceedings, 2006, , .	0.4	0
202	Simulating the Effects of ULF Waves on Energetic Electron Populations. AIP Conference Proceedings, 2006, , .	0.4	0